

# I2VControl: Disentangled and Unified Video Motion Synthesis Control

Wanquan Feng<sup>1†</sup> Tianhao Qi<sup>1,2</sup> Jiawei Liu<sup>1</sup> Mingzhen Sun<sup>1,3</sup> Pengqi Tu<sup>1</sup>  
 Tianxiang Ma<sup>1</sup> Fei Dai<sup>1</sup> Songtao Zhao<sup>1</sup> Siyu Zhou<sup>1</sup> Qian He<sup>1</sup>

<sup>1</sup>ByteDance China <sup>2</sup>University of Science and Technology of China (USTC)

<sup>3</sup>Institute of Automation, Chinese Academy of Sciences (CASIA)

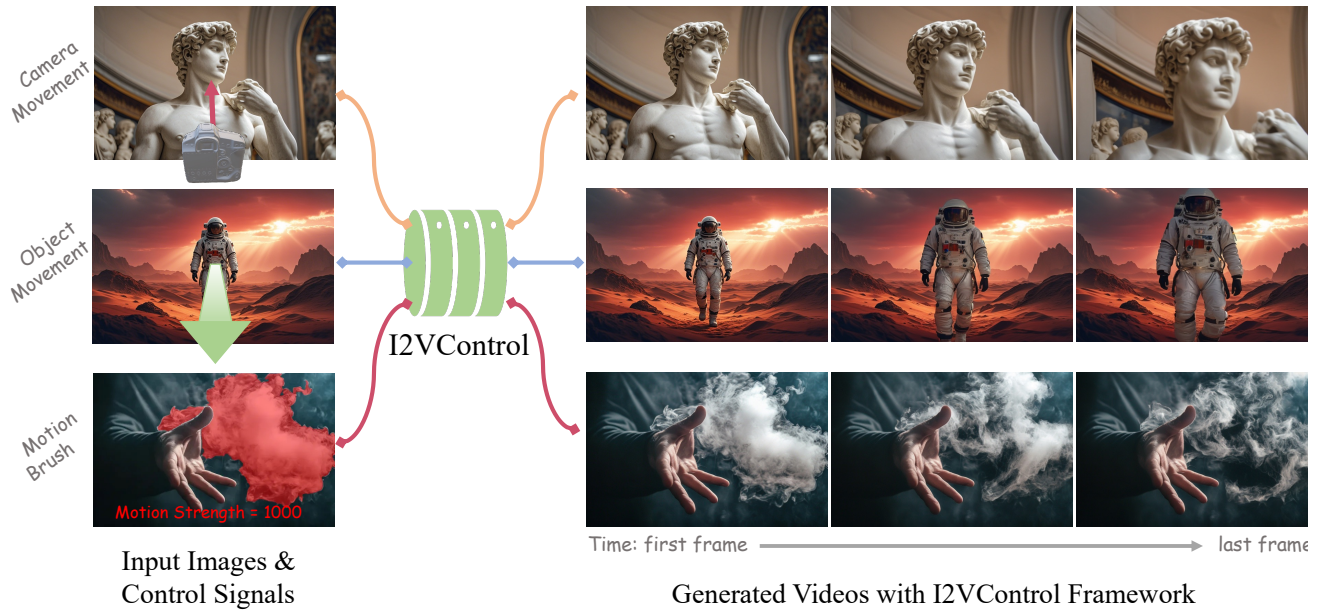


Figure 1. We propose **I2VControl**, an all-in-one unified framework for image-to-video motion synthesis control. In the illustration, we show several scenarios of disentangled controls, including camera movement (camera dollies in and gets closer to the sculpture), object movement (the astronaut walks forward) and motion brush (smoke flows in the wind, with a given motion strength value). **Users can select the control modes according to their requirements, where the control modes can be combined without conflict.**

## Abstract

Video synthesis techniques are undergoing rapid progress, with controllability being a significant aspect of practical usability for end-users. Although text condition is an effective way to guide video synthesis, capturing the correct joint distribution between text descriptions and video motion remains a substantial challenge. In this paper, we present a disentangled and unified framework, namely **I2VControl**, that unifies multiple motion control tasks in image-to-video synthesis. Our approach partitions the video into individual motion units and represents each unit with disentangled control signals, which allows for various control types to be flexibly combined within our single system. Furthermore, our methodology seamlessly integrates as a plugin for pre-trained models and remains agnostic to specific model architectures. We conduct extensive experiments,

achieving excellent performance on various control tasks, and our method further facilitates user-driven creative combinations, enhancing innovation and creativity. The project page is: <https://wanquanf.github.io/I2VControl>.

## 1. Introduction

“The whole is greater than the sum of its parts.”

– Aristotle, *Metaphysics*

Video synthesis technology has significant potential across various fields, such as film production, education, gaming, social media, and advertising. Recently, video synthesis technology has made rapid advancements, with state-of-the-art models like Sora [5], Kling [21] and Vidu [1]

† Corresponding author

achieving outstanding results in generating high-quality video content. In this context, controllability has become crucial for optimizing video production workflows and enhancing content quality, allowing creators to precisely adjust and present their desired visual narratives.

While the integration of text and visual modalities [27] is widely adopted, relying solely on textual conditions to guide video creation poses a significant challenge: the ability to accurately align textual descriptions with the complex motions in videos. This misalignment can lead to a synthesis that strays far from user intentions, ultimately constraining the practical applications of the technology. To address this challenge, prior approaches have attempted to guide the video synthesis process by injecting additional control signals, such as motion drag based control [33, 38] and camera pose control [14, 36]. These approaches, however, often focus on a single type of motion pattern and necessitate the construction of specific data formats tailored for certain scenarios, lacking a comprehensive framework for the integration of multiple control modalities. This limitation proves to be a significant barrier for complex video synthesis tasks. Consequently, these methods, while innovative, do not fully meet the expectations for a satisfactory and intuitive user experience. They often lack the versatility and flexibility required to seamlessly control the video synthesis process, thus providing users with tools that may not be sufficiently adaptable to the wide range of creative demands encountered in video production.

In this paper, we propose a novel video control framework, **I2VControl**, designed to integrate and manage multiple control signals within a single cohesive system. Our framework addresses the limitations of previous methods, which often focus on a single type of motion pattern and require specific data forms. To achieve comprehensive control, we conceptualize the video into trajectory function on individual motion units, each represented by disentangled control signals. Specifically, we categorize the motion units into three types: borderland, drag-units, and brush-units. The borderland units are nearly static, serving as a background with minimal motion. Drag-units are designed for more complex and flexible control, allowing users to manipulate them with six degrees of freedom for precise movement. Brush-units enable control through motion strength values, offering a simpler, yet effective way to influence motion. Trajectory function on each motion unit is further decomposed into a linear term and an additional term, where the decomposition strategy depends on the unit category. By leveraging this detailed structure, I2VControl ensures that each part of the video can be controlled with the desired granularity, from broad strokes to intricate adjustments, meeting the diverse needs of video creators.

For the network structure, we employ a plug-in architecture that equips the video synthesis model with the ca-

pability to fit the aforementioned user interaction process. We also devise a data pipeline to align the training videos with our video representation, streamlining the training process. Our approach allows users to specify various control modalities without logical conflicts, such as camera control, motion brush control, and object dragging, within a unified framework. This flexibility not only enhances the user experience by providing intuitive and precise control but also enables the exploration of combined control methods for richer and more creative video synthesis. Experiments show that our framework achieves excellent flexibility and effectiveness across a diverse range of control scenarios. In summary, our **contributions** include:

- We propose I2VControl, a video motion control framework that unifies multiple control tasks.
- We conceptualize video as motion units and expand trajectory functions on each unit as control signals.
- We develop a plug-in network architecture and a complete data pipeline to conduct the training process.
- Experiments show that our framework not only achieves excellent flexibility and effectiveness but also stimulates user creativity in video production.

## 2. Related Work

### 2.1. Text to Video Synthesis

Text-to-video (T2V) generation is a challenging task that requires both single-modal realism and cross-modal consistency. In the early stage, researchers attempted to solve this task using variational auto-encoders [32], generative adversarial networks [22], and sequential generative models [9, 18, 39, 40]. Despite the progress they made, the performance of these methods was still far from expectations. Recently, diffusion probabilistic models (DPMs) have emerged and boosted the progress of video generation, achieving unprecedented high-quality generation results [3, 5]. Imagen Video [17] and Make-A-Video [30] first generated short videos with low resolutions from texts and then performed spatial super-resolution and temporal interpolation. To reduce the dimensionality of video data, several works [4, 12, 15, 46] introduced video auto-encoders to map videos into low-dimensional latent spaces to reduce computational complexity. VideoLDM [4] extended image auto-encoder to videos. Phenaki [31] proposed a variable-length video auto-encoder using causal attention. Given the lack of high-quality text-video datasets, other researchers conducted text-to-video generation by first generating an image from text and then synthesizing videos from images [10, 23, 34]. MagicVideo-V2 [34] integrated a text-to-image generation model with a video motion generator, reference image embedding module, and frame interpolation module to construct the T2V pipeline. For long T2V generation, StreamingT2V [16] introduced short-term and long-

term memory blocks to enhance video consistency, while NUWA-XL [45] combined a global diffusion to generate coarse video and a local diffusion to generate fine video content, thus obtaining extremely long video generation.

## 2.2. Image to Video Synthesis

Unlike text-to-video (T2V) generation, image-to-video (I2V) generation leverages a static image to define the semantic content while using text prompts to specify and control the motion dynamics within the generated videos. Several approaches have been proposed to maintain the visual fidelity of the original image while introducing realistic and contextually appropriate motion. Most straightforwardly, VideoCrafter1 [6] integrated CLIP embeddings of the static image into DPMs through a dual cross-attention layer akin to IP-Adapter [6]. Meanwhile, I2V-Adapter [11] advanced this technique by establishing interactions between the given image and the subsequent noisy frames via a cross-frame attention mechanism. Notably, Animate Anyone [19] pointed out the loss of fine-grained detail information in CLIP embeddings and creatively adopts an identical network to the DPMs for image condition injection. In contrast, DreamVideo [37] attempted to achieve high-fidelity image-to-video generation by a ControlNet-like structure. Besides, SEINE [7], PixelDance [47], and PIA [49] have independently opted to expand the input channels of DPMs for injecting image information through concatenating the additional image latent with the initial noisy latents, which can better maintain the detail fidelity theoretically and practically. Moreover, several works [2, 41, 48] combined various image condition injection approaches to achieve more fine-grained detail control.

## 2.3. Video Synthesis Controllability

With the development of video generation technology, some video control technologies have also been proposed recently. For camera control, MotionCtrl [36] and CamereC-trl [14] employed an adaptive encoder for the extrinsic matrix of each frame to control the camera movement, and CamCo [42] integrated an epipolar attention module to enforce the 3D-consistent constraints. I2VControl-Camera [8] proposed to control the camera movement with dense trajectory, where a motion strength controller is employed together for adjustive motion dynamic. There are several strategies for object motion control. Boximator [33] and Direct-A-Video [43] utilized the trajectory of the bounding box of the object to guide the object motion. DragN-VWA [44] employed some vector arrows to guide the object movement in the input image. DragAnything [38] further toke use of the explit segmentation infomation constructed by SAM [20] to map the dragging arrow to correct pixel rigions. MOFA-Video [25] employed a sparse-to-dense strategy to convert the user input dragging arrows

into dense flow and thus control the video generation process. Some polular video generation tools, such as Gen-2 [28], and Kling [21] also involved the above functions. In this work, we propose to unify these functions in one single framework, for completely disentagled control.

## 3. Method

In this section, we present details of the **I2VControl** framework. We introduce our video representation in Sec. 3.1, the control signal construction in Sec. 3.2, our network architecture, training and inference process in Sec. 3.3.

### 3.1. Video Representation

In this section, we introduce the video representation used in our paper. We first introduce the motion unit partition, and then define the unit-wise trajectory function.

**Motion Units.** A video can be conceptualized as a sequence of frames in time range  $\lambda \in [0, T]$ , each capturing a projection of a deformable underlying 3D world through a camera with potential camera movement. We denote the domain of 3D points captured by the first frame (at time moment  $\lambda = 0$ ) as  $\Omega \subseteq \mathbb{R}^3$ . Typically, the domain captured by the camera is composed of multiple independent motion parts instead of one total part, which encourages us to divide the entire domain  $\Omega$  into multiple independent ‘‘motion units’’:

$$\Omega = \bigsqcup_{p=0}^P \Omega^{(p)} = \bigsqcup_{p=0}^P (\chi^{(p)} \odot \Omega), \quad (1)$$

where  $p \in \{0, 1, \dots, P\}$  denotes the unit index,  $\Omega^{(p)}$  denotes the  $p$ -th unit,  $\chi^{(p)}$  denotes the mask of the  $p$ -th unit. Based on the properties and control situations, we summarize these units into three categories, defined as: **brush-units**, **drag-units**, and the **borderland**. Both brush-units and drag-units belong to the foreground, and the difference between them lies in the control process. The brush-units are controlled by scalar value motion strength only, while the drag-units can be controlled by 6-DOF (6 degrees of freedom) motion guidance (a rigid transformation within the group  $SE(3)$ ) and additional motion strength. During training, we randomly set a foreground part as one of the two categories. During inference process, the choice is made by the users. The region that are not covered by the brush-units and the drag-units is summarized as a single part, which we call the borderland. During the training and inference process, we always consider the borderland part as the first part with index 0, both the brush-units and the drag-units are assigned indices greater than 0.

**Unit-wise Trajectory Function.** We have introduced the motion unit partition of the captured domain  $\Omega$ . Now, we construct the trajectory function on  $\Omega$  to characterize the motion of the 3D points within it. Without loss of generality, we use the camera coordinate system of the first

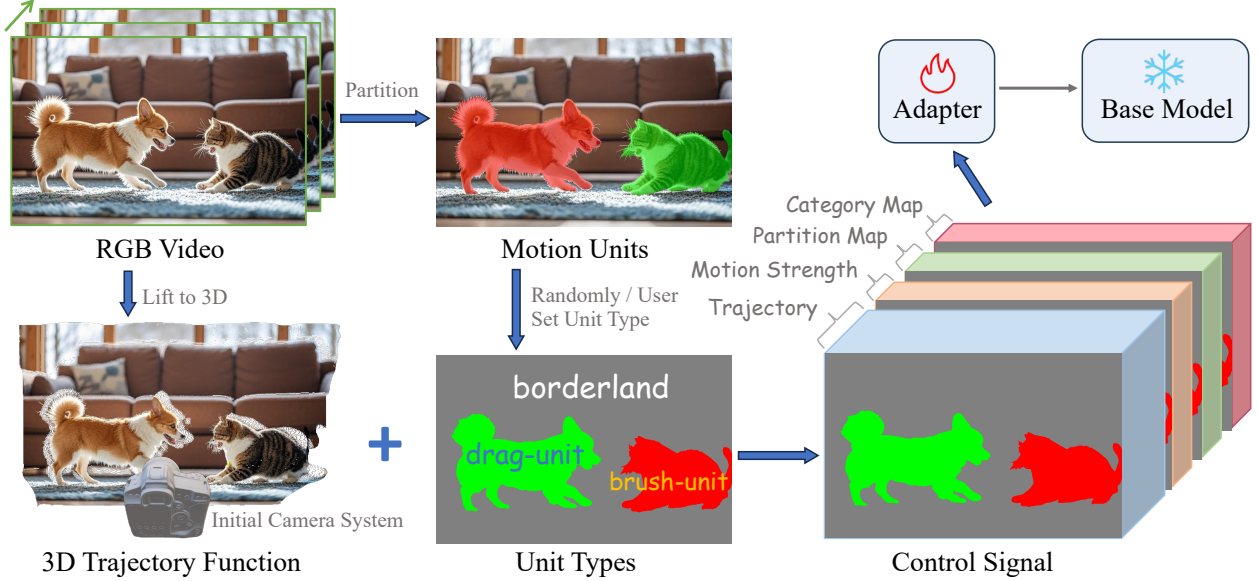


Figure 2. Data pipeline of **I2VControl**. A video is represented as a 3D point trajectory function within the camera system at the initial frame. We perform motion unit partitioning and define the unit-wise trajectory function. Except for the borderland, other units are randomly assigned as either drag- or brush-units. The final control signal includes point trajectory, motion strength, partition and category map.

frame as the world coordinate system. So we can define a trajectory function in the world coordinate system,  $\mathcal{D}(\lambda, \mathbf{x}) : [0, T] \times \Omega \rightarrow \mathbb{R}^3$ , where  $\mathcal{D}(\lambda, \mathbf{x})$  represents the position of the point  $\mathbf{x} \in \Omega$  at time  $\lambda$ . At the initial moment ( $\lambda = 0$ ), the function is simply  $\mathbf{x}$  itself, i.e.,  $\mathcal{D}(0, \mathbf{x}) = \mathbf{x}$ .

To better handle the unit-wise motion, on each unit  $\Omega^{(p)}$ , we decompose the trajectory function into two terms: a rigid term and an additional term:

$$\mathcal{D}(\lambda, \mathbf{x}) = \mathcal{R}_\lambda^{(p)} \circ \mathbf{x} + \mathcal{G}^{(p)}(\lambda, \mathbf{x}), \quad \forall \mathbf{x} \in \Omega^{(p)}, p \in \{0, \dots, P\}, \quad (2)$$

where  $\mathcal{R}_\lambda^{(p)} \in SE(3)$  is a rigid transformation of the initial point set  $\Omega^{(p)}$ , and  $\mathcal{G}^{(p)}(\lambda, \mathbf{x})$  is the additional term showing the difference between  $\mathcal{R}_\lambda^{(p)}$  and  $\mathcal{D}(\lambda, \mathbf{x})$ .

Further, we convert the trajectory function into the camera coordinate system. At each time moment  $\lambda$ , we denote the camera extrinsic as  $\mathcal{E}_\lambda \in SE(3)$ . The transformation from the world coordinate system (i.e., the coordinate system of the first frame) to the camera coordinate system at time  $\lambda$  is given by the inverse of  $\mathcal{E}_\lambda$ , denoted as  $\mathcal{E}_\lambda^{-1}$ . Thus, the transformation of the trajectory function  $\mathcal{D}$  from the world coordinate system to the camera coordinate system can be expressed as:

$$\mathcal{F}(\lambda, \mathbf{x}) = \mathcal{E}_\lambda^{-1} \circ \mathcal{D}(\lambda, \mathbf{x}), \quad (3)$$

where  $\mathcal{F}(\lambda, \mathbf{x})$  represents the position of the point  $\mathbf{x}$  in the camera coordinate system at time  $\lambda$ . Considering that  $\mathcal{E}_0 = \mathcal{I}$ , we can deduce that:

$$\mathcal{F}(0, \mathbf{x}) = \mathcal{E}_0^{-1} \circ \mathcal{D}(0, \mathbf{x}) = \mathcal{I} \circ \mathcal{D}(0, \mathbf{x}) = \mathbf{x}, \quad (4)$$

which proves that  $\mathcal{F}(\lambda, \mathbf{x})$  is still a trajectory function representing the point motions from their initial positions. So the decomposition in Eq. 2 becomes:

$$\mathcal{F}(\lambda, \mathbf{x}) = \mathcal{E}_\lambda^{-1} \circ \mathcal{R}_\lambda^{(p)} \circ \mathbf{x} + \mathcal{E}_\lambda^{-1} \circ \mathcal{G}^{(p)}(\lambda, \mathbf{x}), \quad \forall \mathbf{x} \in \Omega^{(p)}, \quad (5)$$

### 3.2. Control Signal Construction

In this section, we describe how we construct the control signals. We start by defining a general motion strength function in a general setting. Consider an arbitrary domain  $\Gamma \subset \mathbb{R}^3$ , and an arbitrary trajectory function  $\mathcal{H}(\lambda, \mathbf{x}) : [0, T] \times \Gamma \rightarrow \mathbb{R}^3$ , we refer to I2VControl-Camera [8] and define the motion strength function  $\mathcal{M}$  as:

$$\mathcal{M}(\Gamma, \mathcal{H}, \lambda) = \frac{1}{|\Gamma|} \int_{\Gamma} \left\| \frac{\partial \mathcal{H}(\mathbf{x}, \lambda)}{\partial \lambda} \right\|_2 d\mathbf{x}, \quad (6)$$

where the result is a scalar value. An important property to note is that  $\mathcal{M}$  is invariant with respect to rigid transformations on  $\mathcal{H}$ :

$$\mathcal{M}(\Gamma, \mathcal{E} \circ \mathcal{H}, \lambda) \equiv \mathcal{M}(\Gamma, \mathcal{H}, \lambda), \quad \forall \mathcal{E} \in SE(3), \quad (7)$$

which implies that the motion strength is independent of the choice of coordinate system.

Now we describe how we set the  $\mathcal{R}_\lambda^{(p)}$  and motion strength value  $m_\lambda^{(p)}$  on different kinds of units:

- On the **borderland**, we simply set:

$$\mathcal{R}_\lambda^{(p)} \equiv \mathcal{I}, \quad m_\lambda \equiv 0. \quad (8)$$

Note that, despite setting  $m_\lambda$  to 0 during both training and testing, this does not imply that the borderland is completely stationary. On the contrary, it may still exhibit some motion dynamics, ensuring the borderland integrates naturally and seamlessly with the drag-units and brush-units to create a coherent and lifelike video scene. In our constructed training data, the borderland may contain natural small motions, which are also present in the inference results.

- On the **brush-units**, we set:

$$\mathcal{R}_\lambda^{(p)} \equiv \mathcal{I}, \quad m_\lambda = \mathcal{M}(\Omega^{(p)}, \mathcal{G}^{(p)}, \lambda). \quad (9)$$

Similar to the borderland, we set  $\mathcal{R}_\lambda^{(p)} \equiv \mathcal{I}$  on brush-units because we do not require users to provide drag controls for these parts. Instead, users only need to provide the value of  $m_\lambda$ . For the training data, we compute the motion strength with Eq. 6, which indicates the motion deviation from the identity transformation  $\mathcal{I}$ . During inference, users can designate an object by drawing a mask and make it move by simply classifying the region as a brush-unit and providing a motion strength value.

- On the **drag-units**, we set:

$$\mathcal{R}_\lambda^{(p)} = \arg \min_{\mathcal{R} \in SE(3)} \int_{\Omega^{(p)}} \|\mathcal{D}(\lambda, \mathbf{x}) - \mathcal{R} \circ \mathbf{x}\|^2 d\mathbf{x}, \quad (10)$$

$$m_\lambda = \mathcal{M}(\Omega^{(p)}, \mathcal{G}^{(p)}, \lambda). \quad (11)$$

We set  $\mathcal{R}_\lambda^{(p)}$  as the rigid transformation that best “fits” the trajectory, which can be obtained by solving a least-squares problem. In other words,  $\mathcal{R}_\lambda^{(p)}$  serves as a satisfactory “proxy” for the motion in this part. Considering its rigid nature, which can be described using just 6 degrees of freedom, it is also user-friendly. The motion strength  $m_\lambda$  is computed with the same formulation as the brush-units. However, for the drag-units,  $m_\lambda$  indicates the motion deviation from the rigid fitting result instead of the identity transformation. During inference, users can control the motion of an object by drawing its mask, designating the region as a drag-unit, and providing both the rigid transformation and the additional motion strength value.

In addition to the unit-wise definitions, another important control aspect is the camera control, denoted as  $\mathcal{E}_\lambda$ . This control is shared by all units and is also represented as a 6-DOF signal, ensuring user-friendliness. Inspired by I2VControl-Camera, we do not directly employ  $\mathcal{E}_\lambda$  and  $\mathcal{R}_\lambda^{(p)}$  as the control signal. Instead, we use them to compute the **point trajectory** in the camera coordinate system:

$$\mathbf{T}_\lambda = \bigsqcup_{p=0}^P \Pi(\mathcal{E}_\lambda^{-1} \circ \mathcal{R}_\lambda^{(p)} \circ (\chi^{(p)} \odot \Omega)), \quad \lambda \in [0, T], \quad (12)$$

where  $\Pi(\cdot)$  means the projection operation. Further, we or-

ganize the **motion strength map** as:

$$\mathbf{M}_\lambda = \bigsqcup_{p=0}^P (m_\lambda \cdot (\chi^{(p)} \odot \Omega)), \quad \lambda \in [0, T], \quad (13)$$

To pass the unit index into the network, we further construct a **partition map** as:

$$\mathbf{P}_\lambda = \bigsqcup_{p=0}^P (p \cdot (\chi^{(p)} \odot \Omega)), \quad \lambda \in [0, T], \quad (14)$$

Furthermore, it is essential for the network to recognize the category of each unit. We assign  $c^{(p)}$  the values 0, 1, and 2 when the  $p$ -th unit is classified as borderland, drag-part, and brush-part, respectively. Thus, we define a **category map** as:

$$\mathbf{C}_\lambda = \bigsqcup_{p=0}^P (c^{(p)} \cdot (\chi^{(p)} \odot \Omega)), \quad \lambda \in [0, T], \quad (15)$$

Finally, we concatenate the aforementioned control signals together to form the ultimate control signal  $(\mathbf{T}_\lambda, \mathbf{M}_\lambda, \mathbf{P}_\lambda, \mathbf{C}_\lambda)$ .

In our data pipeline, we first apply SAM [20] to partition the first frame image into individual parts. Following the method for obtaining the dynamic mask from I2VControl-Camera, we then extract parts that intersect with the dynamic mask with an intersection area occupying more than half of the total area. These extracted parts are used as our training units, randomly set as drag-unit or brush-unit. All unselected parts are merged into a single borderland. We adhere to the data strategy employed in I2VControl-Camera, tracking  $\mathcal{F}(\lambda, \mathbf{x})$  and solving  $\{\mathcal{E}_\lambda\}_{\lambda \in [0, T]}$ , and then compute  $\mathcal{D}(\lambda, \mathbf{x}) = \mathcal{E}_\lambda \circ \mathcal{F}(\lambda, \mathbf{x})$ . After discretizing the aforementioned variables, our control signal is ultimately represented as a tensor with the shape  $(T, 5, H, W)$ .

### 3.3. Network, Training and Inference

As mentioned above, we apply an adaptive strategy to design the network structure. Taking the  $(T, 5, H, W)$ -shaped tensor as input, we first apply several convolutional layers to convert the input to tokens and then concatenated them with the tokens in the original diffusion process before self-attention computation. After computing self-attention, the additional parts added during concatenation are removed manually to restore the original token shape, following the approach of [19]. The restored token is added back to the original diffusion token, thus completing the adapter calculation process. Except for inserting the above adapter structure, we keep all other training processes consistent with the original base model, including the loss and scheduler.

During inference, we first use the Unidepth [26] metric depth estimation method to obtain the initial point set  $\Omega$ .

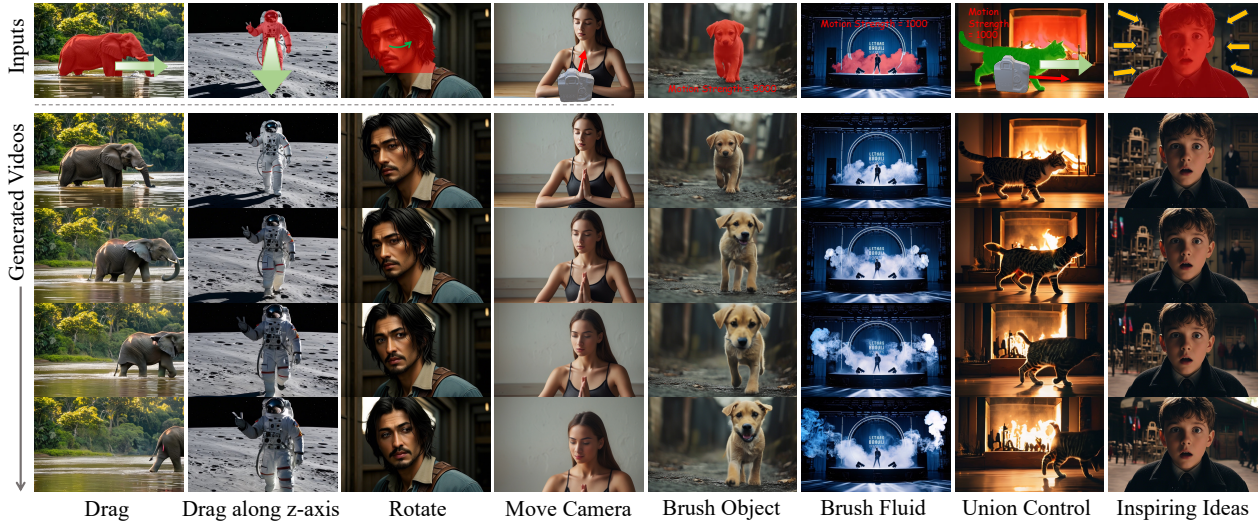


Figure 3. We list some (not all) capabilities of I2VControl. The first two columns illustrate dragging operations within the xy-plane and along the z-axis, respectively. The third column demonstrates rotational capabilities, and the fourth showcases camera movement control. Columns five and six depict motion brush effects. The seventh column presents a combined control including camera movement, dragging, and motion brush. The eighth column shows a creative user idea, a Hitchcockian camera movement, implemented with I2VControl.

Users then interact with our system to provide further input. They can first select the motion units of interest. Specifically, users can employ a bounding box and text description to select a small patch, and then set it as either a brush-unit or a drag-unit. If set as a drag-unit, users are required to provide a 6-DOF input to control the movement of that patch. Users can repeatedly select multiple patches until they have completed their design. Additionally, users can input an overall camera movement, which does not conflict with the motion of the selected patches. Our system provides a preview interface, allowing users to see the results of the drag and camera movement in real-time, achieving a “what you see is what you get” experience, which is highly convenient. After user interaction is complete, we convert the user inputs into control signals and conduct inference.

## 4. Experiments

In this section, we introduce our experiments. Sec. 4.1 presents our implementation details and settings. In Sec. 4.2, we conduct the feature comprehensiveness comparison with previous methods to show the completeness and superiority of our framework design. In Sec. 4.3, we show our results and experimental comparisons. We strongly recommend visiting our project page to view video results: <https://wanquanf.github.io/I2VControl>.

### 4.1. Settings

**Implementation Details.** In this work, we utilize an Image-to-Video variant of the Magicvideo-V2 [35] as our foundational model (24 frames with resolution  $704 \times 448$ ). Training is executed on 16 NVIDIA A100 GPUs, with each GPU

processing a batch size of 1. The entire training spans over 100K steps. Throughout the training phase, we maintain the parameters of the foundational model unchanged while focusing solely on the training of our newly incorporated adapter structure. For comparisons, we test on both motion strength based (motion brush) and motion trajectory based (motion drag, camera movement) tasks.

**Datasets.** We collect a training set of 970K video clips, where each video may contain object motion or camera movement. To test on the motion trajectory based control task, we follow previous work DragAnything [38] and test on the VIPSeg [24] dataset (We selected all samples with at least 24 frames in the testing set of VIPSeg, a total of 101 testing samples). Given that the VIPSeg videos generally lack aesthetic appeal, we think them inadequate for real-world user scenarios. To address this, we invite several real-world users familiar with video creation to construct a manual labelled dataset, which should be more closely aligned with typical user scenarios. Specifically, they employ text-to-image model to generate some high-aesthetic images, and then manually construct the segmentation mask, the camera movement and object motion as the control signal, which completely simulates user operation. To test on the motion trajectory control task, we collect 30 labelled samples with movable objects. Similarly, to test on the motion strength based control task, we construct a dataset of 63 testing samples, 33 of which are object motion (e.g., humans, animals) and the other 30 are fluid effects (e.g., smoke, fire).

**Metrics.** For the motion trajectory control task, we refer to DragAnything [38] and TrackGo [13], evaluating the quality of the results by ObjMC. Note that since we allow control via dense trajectories instead of sparse control points,

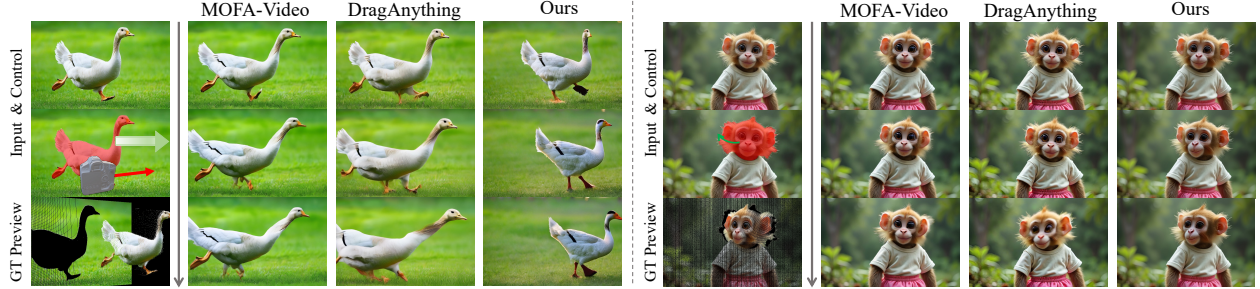


Figure 4. Comparison on trajectory control task.

	Motion Drag	Camera Extrinsics	Motion Brush
Boximator [33]	✓	✗	✗
MotionCtrl [36]	✓	✓	✗
CameraCtrl [14]	✗	✓	✗
DragNUWA [44]	✓	✗	✗
DragAnything [38]	✓	✗	✗
Motion-I2V [29]	✓	✗	✓
MOFA-Video [25]	✓	✗	✗
TrackGo [13]	✓	✗	✗
I2VControl (Ours)	✓	✓	✓

Table 1. Feature Comprehensiveness Comparison.

we compute this metric on dense trajectories. To evaluate motion brush control task, we firstly compute a motion strength score, denoted as MSC, as in I2VControl-Camera. Then we refer to SAM [20] to employ a  $\text{IoU}$  metric to evaluate whether the generated motion follows the user input mask. Moreover, for all experiments, we additionally compute the FID score to measure the quality of the results.

## 4.2. Feature Comprehensiveness Analysis

In this section, we theoretically compare the feature comprehensiveness between our method and some very recent baseline methods in Tab. 1. We mainly focus on the following control strategies: motion drag, camera extrinsics, and motion brush, all of which are important components of popular video generation commercial products, such as Gen2 [28]. For **motion drag**, users can select some points/objects on the input image and drag them to target positions, thus guide the video generation process. For **camera extrinsics** control, users are allowed to set a camera pose sequence to decide the camera movement of the generated video. For **motion brush**, we adopt the definition from motion-I2V [29], which enables the selected region to move (without specifying a trajectory or direction), while not affecting other unselected areas. From Tab. 1, we can see that only our method can deal with all the above common control situations in one single framework.

It is noteworthy that although some motion drag methods (e.g. DragAnything [38], MOFA-Video [25]) do not accept

a camera matrix as input, they propose that the effect of camera movement can be achieved by applying 2D drags to multiple points in the background. This also reminds us that both camera movement and motion drag can essentially be considered as 2D trajectory based control, where the former acts on the background and the latter on the subject. In the following sections, we conduct comparisons in two major categories: trajectory based control and motion brush.

## 4.3. Results and Comparisons

In this section, we present our experimental results and comparisons with previous methods. Secondly, in Sec. 4.3.1, we show the diverse capabilities of our framework by applying it on several inspiring and creative control situations. In order to form a more convincing experiment, we compare with other methods on trajectory based control in Sec. 4.3.2 and motion brush in Sec. 4.3.3.

### 4.3.1. Diverse Capabilities and Creative Exploration

As an disentangled and unified framework, I2VControl can combine multiple spatial control ideas without conflict, which can greatly meet the needs of video creation users. We show some examples in Fig. 3. The first three columns represent several situations of 6-DOF object movement, including basic translation and rotation. Note that the second column is a translation along the Z-axis, and the third column is the rotation of the head, which are difficult to achieve in previous methods. The fourth column shows an arbitrary camera movement. The fifth and sixth columns are motion brushes for objects and fluids, respectively. In the seventh column, we show a combined effect, where the camera and object movements, and the motion strength based brush are employed in one single sample. The eighth column shows a creative control from user idea. Specifically, we keep the foreground still and the background zoomed out, making it look like the background is quickly moving backwards (the Hitchcockian camera movement). Due to constraints on time and page space, we did not show more inspiring ideas. However, the examples provided sufficiently demonstrate that our system empowers users with the tools they need to unleash their creativity, encouraging them to explore and devise more intriguing control combinations.

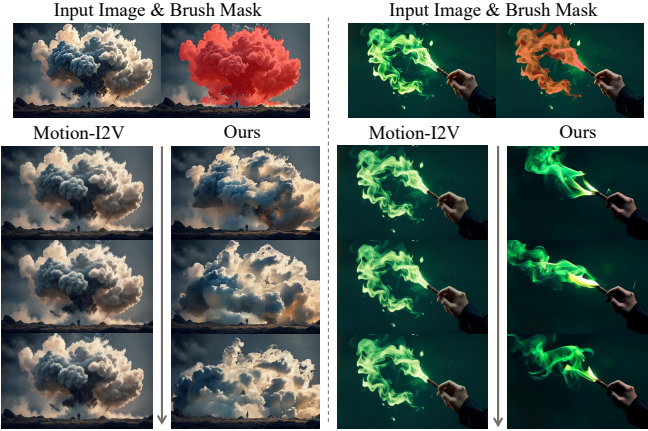


Figure 5. Comparison on motion brush for fluid effects.

#### 4.3.2. Comparison on Trajectory Control

We compare on the trajectory control based task (including object motion and camera movement) with very recent methods DragAnything [38] and MOFA-Video [25]. As described in Sec. 4.1, we test on the VIPSeg [24] dataset and another manual dataset. For each sample, we divide the motion units on the initial frame. To construct the control signal for the comparing methods, we extract representative trajectories on each single units, where one trajectory is selected for the drag-units and four trajectories are selected for the borderland part to represent the camera movement. Quantitatively, we calculate the metric between the generated results and the ground truth control signals, and show the results on both datasets in Tab. 2. Compared to previous methods, we achieve better results on both VIPSeg and the manual dataset and both the ObjMC and FID metrics, which shows that our method is superior to previous methods on both controlling precision and fidelity. The qualitative results can be seen in Fig. 4. In the left sample, we use a pan-right camera movement and drag the object to the right, and only our result is right, thanks to our dense and disentangled nature. The sample on the right shows our good performance for rotation control.

Dataset	Metric	DragAnything	MOFA-Video	Ours
VIPSeg	ObjMC↓	211.01	239.76	<b>197.60</b>
	FID↓	136.56	141.50	<b>127.44</b>
Manual	ObjMC↓	31.24	43.60	<b>17.07</b>
	FID↓	235.31	251.78	<b>226.08</b>

Table 2. Comparison on the trajectory control task.

#### 4.3.3. Comparison on Motion Brush

We compare on the motion brush control task, where we brush masks on images and set scalar motion strength for the selected region without a motion trajectory or direction

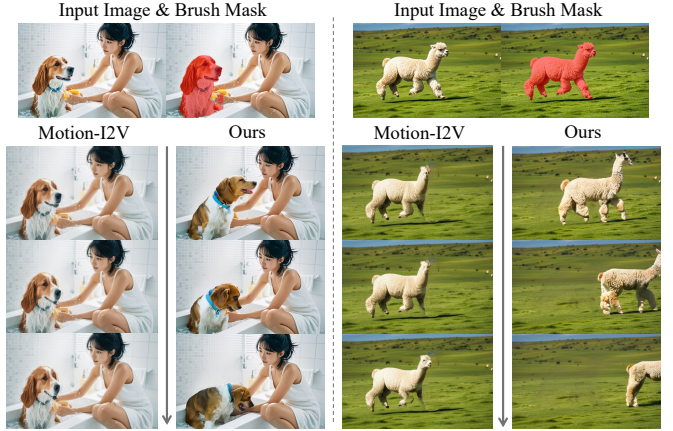


Figure 6. Comparison on motion brush for object movements.

guide. As described in Sec. 4.1, we test on two types of inputs, the movable objects and fluid effects. We outperform previous method Motion-I2V on both datasets and all metrics (see Tab. 3), reflecting our effectiveness better response to masks and more significant motion. The numerical difference is very intuitively reflected in the visualization results, see Fig. 6 and Fig. 5. The result of Motion-I2V has a small motion range, and the movable pixels seems not able to move out of the given mask. This might be related to the control strategy based on optical flow. In contrast, our method can produce very large-scale motion. For example, in Fig. 5, the flame emitted from the wand can be transformed into different shapes. The brushed objects can also move away from the origin mask, such as the animal on the right of Fig. 6.

Datasets	Object Movements		Fluid Effects	
	Motion-I2V	Ours	Motion-I2V	Ours
MSC↑	6.87	<b>64.59</b>	2.57	<b>97.29</b>
IoU (%)↑	15.43	<b>60.34</b>	5.60	<b>46.37</b>
FID↓	246.92	<b>207.68</b>	266.39	<b>223.22</b>

Table 3. Comparison on the motion brush control task.

## 5. Conclusion

In this work, we explore the controllability of video synthesis, a vital aspect for enhancing end-user utility. Our proposed framework, **I2VControl**, implements flexible video motion controllers with disentangled control signals, achieving a user-friendly interface and outstanding performance in various motion control tasks including motion strength, motion brushing, object dragging, and camera pose controlling. For the future, we aim to enhance the framework to handle increasingly complex scenarios, integrating more nuanced control over video motion not only at the structural but also at the textual level. Additionally, we

also expect ongoing advancements in model architectures to boost the capabilities and operational efficiency of our framework.

## Acknowledgement

We thank Yuxi Xiao and Yudong Guo for their generous help and advice with the tracking algorithm.

## References

- [1] Fan Bao, Chendong Xiang, Gang Yue, Guande He, Hongzhou Zhu, Kaiwen Zheng, Min Zhao, Shilong Liu, Yaole Wang, and Jun Zhu. Vidu: a highly consistent, dynamic and skilled text-to-video generator with diffusion models, 2024. 1
- [2] Andreas Blattmann, Tim Dockhorn, Sumith Kulal, Daniel Mendelevitch, Maciej Kilian, Dominik Lorenz, Yam Levi, Zion English, Vikram Voleti, Adam Letts, et al. Stable video diffusion: Scaling latent video diffusion models to large datasets. *arXiv preprint arXiv:2311.15127*, 2023. 3
- [3] Andreas Blattmann, Tim Dockhorn, Sumith Kulal, Daniel Mendelevitch, Maciej Kilian, Dominik Lorenz, Yam Levi, Zion English, Vikram Voleti, Adam Letts, et al. Stable video diffusion: Scaling latent video diffusion models to large datasets. *arXiv preprint arXiv:2311.15127*, 2023. 2
- [4] Andreas Blattmann, Robin Rombach, Huan Ling, Tim Dockhorn, Seung Wook Kim, Sanja Fidler, and Karsten Kreis. Align your latents: High-resolution video synthesis with latent diffusion models. In *Proceedings of the IEEE/CVF Conference on Computer Vision and Pattern Recognition*, pages 22563–22575, 2023. 2
- [5] Tim Brooks, Bill Peebles, Connor Holmes, Will DePue, Yufei Guo, Li Jing, David Schnurr, Joe Taylor, Troy Luhman, Eric Luhman, Clarence Ng, Ricky Wang, and Aditya Ramesh. Video generation models as world simulators. 2024. 1, 2
- [6] Haoxin Chen, Menghan Xia, Yingqing He, Yong Zhang, Xiaodong Cun, Shaoshu Yang, Jinbo Xing, Yaofang Liu, Qifeng Chen, Xintao Wang, et al. Videocrafter1: Open diffusion models for high-quality video generation. *arXiv preprint arXiv:2310.19512*, 2023. 3
- [7] Xinyuan Chen, Yaohui Wang, Lingjun Zhang, Shaobin Zhuang, Xin Ma, Jiashuo Yu, Yali Wang, Dahua Lin, Yu Qiao, and Ziwei Liu. Seine: Short-to-long video diffusion model for generative transition and prediction. In *The Twelfth International Conference on Learning Representations*, 2023. 3
- [8] Wanquan Feng, Jiawei Liu, Pengqi Tu, Tianhao Qi, Mingzhen Sun, Tianxiang Ma, Songtao Zhao, Siyu Zhou, and Qian He. I2vcontrol-camera: Precise video camera control with adjustable motion strength. 2024. 3, 4
- [9] Songwei Ge, Thomas Hayes, Harry Yang, Xi Yin, Guan Pang, David Jacobs, Jia-Bin Huang, and Devi Parikh. Long video generation with time-agnostic vqgan and time-sensitive transformer. In *European Conference on Computer Vision*, pages 102–118. Springer, 2022. 2
- [10] Rohit Girdhar, Mannat Singh, Andrew Brown, Quentin Duval, Samaneh Azadi, Sai Saketh Rambhatla, Akbar Shah, Xi Yin, Devi Parikh, and Ishan Misra. Emu video: Factorizing text-to-video generation by explicit image conditioning. *arXiv preprint arXiv:2311.10709*, 2023. 2
- [11] Xun Guo, Mingwu Zheng, Liang Hou, Yuan Gao, Yufan Deng, Pengfei Wan, Di Zhang, Yufan Liu, Weiming Hu, Zhengjun Zha, et al. I2v-adapter: A general image-to-video adapter for diffusion models. In *ACM SIGGRAPH 2024 Conference Papers*, pages 1–12, 2024. 3
- [12] Agrim Gupta, Lijun Yu, Kihyuk Sohn, Xiuye Gu, Meera Hahn, Li Fei-Fei, Irfan Essa, Lu Jiang, and José Lezama. Photorealistic video generation with diffusion models. *arXiv preprint arXiv:2312.06662*, 2023. 2
- [13] Zhou Haitao, Wang Chuang, Nie Rui, Lin Jinxiao, Yu Dongdong, Yu Qian, and Wang Changhu. Trackgo: A flexible and efficient method for controllable video generation. 2024. 6, 7
- [14] Hao He, Yinghao Xu, Yuwei Guo, Gordon Wetzstein, Bo Dai, Hongsheng Li, and Ceyuan Yang. Cameractrl: Enabling camera control for text-to-video generation. *arXiv preprint arXiv:2404.02101*, 2024. 2, 3, 7
- [15] Yingqing He, Tianyu Yang, Yong Zhang, Ying Shan, and Qifeng Chen. Latent video diffusion models for high-fidelity long video generation. *arXiv preprint arXiv:2211.13221*, 2022. 2
- [16] Roberto Henschel, Levon Khachatryan, Daniil Hayrapetyan, Hayk Poghosyan, Vahram Tadevosyan, Zhangyang Wang, Shant Navasardyan, and Humphrey Shi. Streamingt2v: Consistent, dynamic, and extendable long video generation from text. *arXiv preprint arXiv:2403.14773*, 2024. 2
- [17] Jonathan Ho, William Chan, Chitwan Saharia, Jay Whang, Ruiqi Gao, Alexey Gritsenko, Diederik P Kingma, Ben Poole, Mohammad Norouzi, David J Fleet, et al. Imagen video: High definition video generation with diffusion models. *arXiv preprint arXiv:2210.02303*, 2022. 2
- [18] Wenyi Hong, Ming Ding, Wendi Zheng, Xinghan Liu, and Jie Tang. Cogvideo: Large-scale pretraining for text-to-video generation via transformers. *arXiv preprint arXiv:2205.15868*, 2022. 2
- [19] Li Hu. Animate anyone: Consistent and controllable image-to-video synthesis for character animation. In *Proceedings of the IEEE/CVF Conference on Computer Vision and Pattern Recognition*, pages 8153–8163, 2024. 3, 5
- [20] Alexander Kirillov, Eric Mintun, Nikhila Ravi, Hanzi Mao, Chloe Rolland, Laura Gustafson, Tete Xiao, Spencer Whitehead, Alexander C. Berg, Wan-Yen Lo, Piotr Dollár, and Ross Girshick. Segment anything. *arXiv:2304.02643*, 2023. 3, 5, 7
- [21] KuaiShou. Kling, 2024. 1, 3
- [22] Yitong Li, Martin Min, Dinghan Shen, David Carlson, and Lawrence Carin. Video generation from text. In *Proceedings of the AAAI conference on artificial intelligence*, 2018. 2
- [23] Kangfu Mei and Vishal Patel. Vidm: Video implicit diffusion models. In *Proceedings of the AAAI conference on artificial intelligence*, pages 9117–9125, 2023. 2

[24] Jiaxu Miao, Xiaohan Wang, Yu Wu, Wei Li, Xu Zhang, Yun-chao Wei, and Yi Yang. Large-scale video panoptic segmentation in the wild: A benchmark. In *Proceedings of the IEEE Conference on Computer Vision and Pattern Recognition*, 2022. 6, 8

[25] Muyao Niu, Xiaodong Cun, Xintao Wang, Yong Zhang, Ying Shan, and Yinqiang Zheng. Mofa-video: Controllable image animation via generative motion field adaptions in frozen image-to-video diffusion model. *arXiv preprint arXiv:2405.20222*, 2024. 3, 7, 8

[26] Luigi Piccinelli, Yung-Hsu Yang, Christos Sakaridis, Mattia Segu, Siyuan Li, Luc Van Gool, and Fisher Yu. UniDepth: Universal monocular metric depth estimation. In *Proceedings of the IEEE/CVF Conference on Computer Vision and Pattern Recognition (CVPR)*, 2024. 5

[27] Alec Radford, Jong Wook Kim, Chris Hallacy, Aditya Ramesh, Gabriel Goh, Sandhini Agarwal, Girish Sastry, Amanda Askell, Pamela Mishkin, Jack Clark, Gretchen Krueger, and Ilya Sutskever. Learning transferable visual models from natural language supervision. 2021. 2

[28] Runway. Gen2, 2023. 3, 7

[29] Xiaoyu Shi, Zhaoyang Huang, Fu-Yun Wang, Weikang Bian, Dasong Li, Yi Zhang, Manyuan Zhang, Ka Chun Cheung, Simon See, Hongwei Qin, et al. Motion-i2v: Consistent and controllable image-to-video generation with explicit motion modeling. *SIGGRAPH 2024*, 2024. 7

[30] Uriel Singer, Adam Polyak, Thomas Hayes, Xi Yin, Jie An, Songyang Zhang, Qiyuan Hu, Harry Yang, Oron Ashual, Oran Gafni, et al. Make-a-video: Text-to-video generation without text-video data. *arXiv preprint arXiv:2209.14792*, 2022. 2

[31] Ruben Villegas, Mohammad Babaeizadeh, Pieter-Jan Kindermans, Hernan Moraldo, Han Zhang, Mohammad Taghi Saffar, Santiago Castro, Julius Kunze, and Dumitru Erhan. Phenaki: Variable length video generation from open domain textual descriptions. In *International Conference on Learning Representations*, 2022. 2

[32] Jacob Walker, Ali Razavi, and Aäron van den Oord. Predicting video with vqvae. *arXiv preprint arXiv:2103.01950*, 2021. 2

[33] Jiawei Wang, Yuchen Zhang, Jiaxin Zou, Yan Zeng, Guoqiang Wei, Liping Yuan, and Hang Li. Boximator: Generating rich and controllable motions for video synthesis, 2024. 2, 3, 7

[34] Weimin Wang, Jiawei Liu, Zhijie Lin, Jiangqiao Yan, Shuo Chen, Chetwin Low, Tuyen Hoang, Jie Wu, Jun Hao Liew, Hanshu Yan, et al. Magicvideo-v2: Multi-stage high-aesthetic video generation. *arXiv preprint arXiv:2401.04468*, 2024. 2

[35] Weimin Wang, Jiawei Liu, Zhijie Lin, Jiangqiao Yan, Shuo Chen, Chetwin Low, Tuyen Hoang, Jie Wu, Jun Hao Liew, Hanshu Yan, et al. Magicvideo-v2: Multi-stage high-aesthetic video generation. *arXiv preprint arXiv:2401.04468*, 2024. 6

[36] Zhouxia Wang, Ziyang Yuan, Xintao Wang, Tianshui Chen, Menghan Xia, Ping Luo, and Yin Shan. Motionctrl: A unified and flexible motion controller for video generation. 2023. 2, 3, 7

[37] Yujie Wei, Shiwei Zhang, Zhiwu Qing, Hangjie Yuan, Zhiheng Liu, Yu Liu, Yingya Zhang, Jingren Zhou, and Hongming Shan. Dreamvideo: Composing your dream videos with customized subject and motion. In *Proceedings of the IEEE/CVF Conference on Computer Vision and Pattern Recognition*, pages 6537–6549, 2024. 3

[38] Yuchao Gu, Rui Zhao, Yefei He, David Junhao Zhang, Mike Zheng, Shou Yan, Li Tingting, Gao Di, Zhang Weijia, Wu, Zhuang Li. Draganything: Motion control for anything using entity representation, 2024. 2, 3, 6, 7, 8

[39] Chenfei Wu, Lun Huang, Qianxi Zhang, Binyang Li, Lei Ji, Fan Yang, Guillermo Sapiro, and Nan Duan. Godiva: Generating open-domain videos from natural descriptions. *arXiv preprint arXiv:2104.14806*, 2021. 2

[40] Chenfei Wu, Jian Liang, Lei Ji, Fan Yang, Yuejian Fang, Daxin Jiang, and Nan Duan. Nüwa: Visual synthesis pre-training for neural visual world creation. In *European conference on computer vision*, pages 720–736, 2022. 2

[41] Jinbo Xing, Menghan Xia, Yong Zhang, Haoxin Chen, Xintao Wang, Tien-Tsin Wong, and Ying Shan. Dynamicrafter: Animating open-domain images with video diffusion priors. *arXiv preprint arXiv:2310.12190*, 2023. 3

[42] Dejia Xu, Weili Nie, Chao Liu, Sifei Liu, Jan Kautz, Zhangyang Wang, and Arash Vahdat. Camco: Camera-controllable 3d-consistent image-to-video generation. *arXiv preprint arXiv:2406.02509*, 2024. 3

[43] Shiyuan Yang, Liang Hou, Haibin Huang, Chongyang Ma, Pengfei Wan, Di Zhang, Xiaodong Chen, and Jing Liao. Direct-a-video: Customized video generation with user-directed camera movement and object motion. *arXiv preprint arXiv:2402.03162*, 2024. 3

[44] Shengming Yin, Chenfei Wu, Jian Liang, Jie Shi, Houqiang Li, Gong Ming, and Nan Duan. Dragnuwa: Fine-grained control in video generation by integrating text, image, and trajectory, 2023. 3, 7

[45] Shengming Yin, Chenfei Wu, Huan Yang, Jianfeng Wang, Xiaodong Wang, Minheng Ni, Zhengyuan Yang, Linjie Li, Shuguang Liu, Fan Yang, et al. Nuwa-xl: Diffusion over diffusion for extremely long video generation. *arXiv preprint arXiv:2303.12346*, 2023. 3

[46] Sihyun Yu, Kihyuk Sohn, Subin Kim, and Jinwoo Shin. Video probabilistic diffusion models in projected latent space. In *Proceedings of the IEEE/CVF conference on computer vision and pattern recognition*, pages 18456–18466, 2023. 2

[47] Yan Zeng, Guoqiang Wei, Jiani Zheng, Jiaxin Zou, Yang Wei, Yuchen Zhang, and Hang Li. Make pixels dance: High-dynamic video generation. In *Proceedings of the IEEE/CVF Conference on Computer Vision and Pattern Recognition*, pages 8850–8860, 2024. 3

[48] Shiwei Zhang, Jiayu Wang, Yingya Zhang, Kang Zhao, Hangjie Yuan, Zhiwu Qin, Xiang Wang, Deli Zhao, and Jingren Zhou. I2vgen-xl: High-quality image-to-video synthesis via cascaded diffusion models. *arXiv preprint arXiv:2311.04145*, 2023. 3

[49] Yiming Zhang, Zheneng Xing, Yanhong Zeng, Youqing Fang, and Kai Chen. Pia: Your personalized image animator

via plug-and-play modules in text-to-image models. In *Proceedings of the IEEE/CVF Conference on Computer Vision and Pattern Recognition*, pages 7747–7756, 2024. 3